Process Tomography of Dynamical Decoupling in a Dense Cold Atomic Ensemble

Yoav Sagi, Ido Almog, and Nir Davidson
Department of Physics of Complex Systems, Weizmann Institute of Science, Rehovot 76100, Israel
(Received 12 April 2010; published 27 July 2010)

Atomic ensembles have many potential applications in quantum information science. Owing to collective enhancement, working with ensembles at high densities increases the efficiency of quantum operations, but at the same time also increases the collision rate and leads to decoherence. Here we report on experiments with optically trapped ^{87}Rb atoms demonstrating a 20-fold increase of the coherence time when a dynamical decoupling sequence with more than 200 pi pulses is applied. Using quantum process tomography we demonstrate that a dense ensemble with an optical depth of 230 can be used as an atomic memory with coherence times exceeding 3 seconds.

DOI: 10.1103/PhysRevLett.105.053201 PACS numbers: 34.50.Cx, 03.65.Yz, 03.67.−a, 82.56.Jn

Cold atomic ensembles can be used as an interface between matter and photonic qubits in quantum networks [1,2], and in recent years vast experimental advances in this direction have been reported [3–8]. Quantum information, which is mapped into the coherence between two atomic internal states, is gradually lost due to inhomogeneities and fluctuations in the energy difference between these states. For trapped atoms the inhomogeneities are caused by differential light shift in optical traps [9] or by differential Zeeman shifts in magnetic traps, and by mean-field density dependent interaction shifts [10]. Fluctuations arise due to collisions which are inherent to the high densities required to achieve a good overall efficiency of quantum operations [11,12].

Though fluctuations at low frequencies can be overcome by a single population inverting pulse—the celebrated coherence echo technique [13,14]—as the collision rate increases this is no longer possible due to higher frequency components. Dynamical decoupling (DD) theories generalize this technique to multipulse sequences by harnessing symmetry properties of the coupling Hamiltonian [15–19]. Though DD was demonstrated in several experiments [20–25], its use with atomic ensembles remains unexplored. Here we study experimentally DD in a dense cold atomic ensemble and report on a substantial suppression of collisional decoherence. We also find that although the ensemble is a non-Gaussian many-body system which is almost decoupled from the environment, the coherence time with DD is described well by an effective single spin coupled to a Gaussian reservoir.

We consider atoms with internal states $|1\rangle$ and $|2\rangle$, trapped in a conservative optical potential. An effective single particle Hamiltonian is given by

$$\hat{H} = \hbar[\omega_0 + \delta(t)]|2\rangle\langle 2| + \hbar\Omega(t)|2\rangle\langle 1| + \text{H.c.}, \quad (1)$$

where ω_0 is the free space transition frequency between the states, $\delta(t)$ is a random frequency detuning sequence whose nature is determined by the potential inhomogeneities and collisions, and $\Omega(t)$ is the external control field which is used for the DD. Starting with an initial state $|\psi(0)\rangle = 2^{-1/2}(|1\rangle + |2\rangle)$ and no external control fields, the wave function at any given time is given in the rotating frame by $|\psi(t)\rangle = 2^{-1/2}(|1\rangle + e^{-i\phi(t)}|2\rangle)$, where the phase difference is given by $\phi(t) = \int_0^t \delta(t)dt$. A schematic plot of three realizations of $\phi(t)$ is given in Fig. 1(a), and it can be seen that the phase difference is accumulated in a constant rate between collisions [26]. The ensemble coherence is characterized by the function $C(t) = \frac{|\langle\rho_{12}(t)\rangle|}{|\langle\rho_{12}(0)\rangle|}$, where

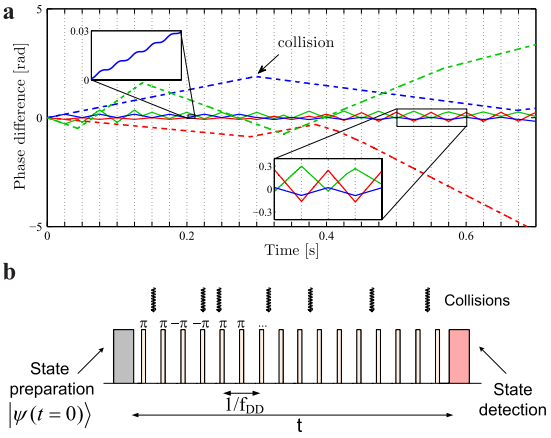

FIG. 1 (color online). (a) Schematic drawing of the relative phase between the two internal states for three atomic realizations. Without dynamical decoupling (dashed lines), the average detuning, $\delta(t)$, is changed after each collision. With DD pulses (dotted vertical lines) the spread of the atomic phases is much smaller (solid lines). The upper inset shows small oscillations due to the fast periodic atomic motion in the trap. Since the oscillation period is shorter than all relevant time scales in our experiment, we consider only $\delta(t)$ averaged over an oscillation period [26]. (b) The experimental pulse sequence starts with a state preparation, followed by a train of π pulses with alternated phases to minimize the accumulation of errors due to pulse width and frequency inaccuracies, and a final state detection. The duration of each π pulse is ~0.5 ms and its average fidelity is ~0.995.

ρ_{12} is the off-diagonal element of the reduced two-level density matrix [19]. As an example, for a Gaussian phase distribution, P_ϕ, with a standard deviation σ_ϕ, we obtain $C(t) = e^{-\sigma_\phi^2(t)/2}$, which shows that the coherence decays as the width of the phase distribution increases. The effect of a population inverting pulse (π pulse) is to change the sign of δ, and a train of such pulses lead to a much narrower phase distribution and slower decoherence [solid lines in Fig. 1(a)].

The experiments are carried out with laser cooled ^{87}Rb atoms trapped by two far-off-resonance laser beams with a wavelength of 1064 nm crossing at an angle of 28° [27]. The two relevant internal states are $|1\rangle = |F = 1; m_f = -1\rangle$ and $|2\rangle = |F = 2; m_f = 1\rangle$ in the $5^2S_{1/2}$ manifold, which are to first order Zeeman insensitive to magnetic fluctuations in the applied magnetic field of 3.2 G [10]. The external control is done by means of two-photon transition (MW-rf photons). We measure the internal state of the atoms by a fluorescence detection scheme [27,28], and their density and temperature using absorption imaging on a CCD camera. By gradually lowering the trapping laser intensity we reach the experimental conditions, at which there are typically 275 000 atoms at a temperature of 1.7 μK, phase space density of 0.04, average collision rate of 100 sec^{-1}, and radial and axial oscillation frequencies of $\omega_r = 2\pi \times 330$ Hz and $\omega_a = 2\pi \times 87$ Hz, respectively. The typical inhomogeneous decay time as measured in a Ramsey-like experiment is ~150 msec. The peak optical depth for a nonpolarized resonant light is ~230.

We employ a Carr-Purcell-Meiboom-Gill (CPMG) decoupling scheme [29] and show in what follows that for collisional detuning fluctuations it is virtually optimal. The pulse sequence is composed of n π pulses at times $t_k = \frac{2k-1}{2n}t$ where $k = 1 \ldots n$ [see Fig. 1(b)], and we characterize it by its effective Rabi frequency $f_{\mathrm{DD}} = \frac{n}{2t}$. We study the effect of the DD scheme by performing a quantum process tomography (QPT). QPT enables us to reconstruct the χ matrix which gives a convenient way to calculate the density matrix after the process, ρ_{out}, in terms of the initial density matrix, ρ_{in}, by $\rho_{\mathrm{out}} = \mathcal{E}[\rho_{\mathrm{in}}] = \sum_{k,l}\hat{E}_k\rho_{\mathrm{in}}\hat{E}_l^\dagger\chi_{kl}$, where $\hat{\mathbf{E}} = (\hat{I}, \hat{X}, -i\hat{Y}, \hat{Z})$ with $(\hat{I}, \hat{X}, \hat{Y}, \hat{Z})$ being the Pauli matrices. In the experiment we start with a set of initial states after which we apply the decoupling scheme and measure ρ_{out} by quantum state tomography (for more details see the supplementary material [27]). The results of a QPT of a DD sequence with $f_{\mathrm{DD}} = 35$ Hz is depicted in Fig. 2. There are two distinctive decay time scales for the equatorial plane and the z axis, which corresponds to phase damping noise processes and depolarizing noise processes (T_1), respectively. The former originates from collisional fluctuations in δ and it is the dominant noise process which determines the ensemble coherence time, τ_c, which is quantified by $C(t)$. The depolarization process is induced by inelastic collisions, and its typical time scale is measured to be $T_1 = 6$ s [30]. The worst case fidelity of the ensemble as a quantum memory, defined as $\mathcal{F} = \min_{|\psi\rangle}\langle\psi|\mathcal{E}[|\psi\rangle\langle\psi|]|\psi\rangle$, is calculated from the measured χ matrix to be $\mathcal{F} = 0.83$, 0.74, and 0.64 for 1, 2, and 3 seconds, respectively, which corresponds to an exponential decay time scale of $\tau_c = 2.4$ sec. The contraction of the Bloch sphere is symmetric in the equatorial plane, which indicates that the decoupling scheme is insensitive to the stored superposition. We demonstrate this point with a direct measurement in which we start with two orthogonal initial states in the equatorial plain and scan the phase of a final $\pi/2$ pulse added to the sequence and measure the population at $|2\rangle$ normalized to its initial value. The results depicted in the inset of Fig. 3 exhibit the same contrast and preserve the $\pi/2$ phase shift between the two initial states.

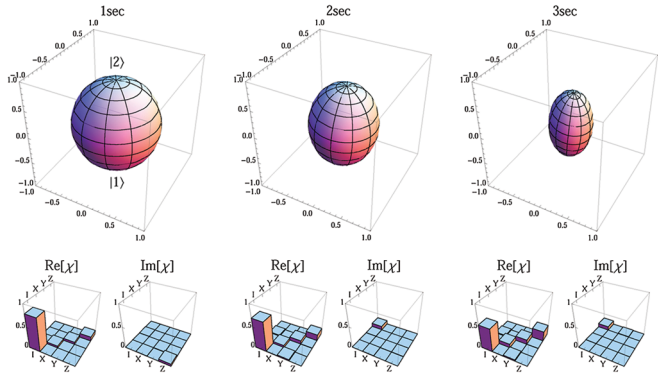

FIG. 2 (color online). Quantum process tomography of dynamical decoupling with $f_{\mathrm{DD}} = 35$ Hz. Any single-qubit density matrix ρ can be mapped to a point in space $\vec{r}(\rho) = [\mathrm{tr}(\hat{X}\rho), \mathrm{tr}(\hat{Y}\rho), \mathrm{tr}(\hat{Z}\rho)]$, with $(\hat{X}, \hat{Y}, \hat{Z})$ being the Pauli matrices. The colors and lines are chosen for the initial states, ρ_{in}, which lie on a sphere with a radius 1. For each of these states we calculate the process outcome, $\rho_{\mathrm{out}} = \mathcal{E}[\rho_{\mathrm{in}}]$, and plot it with its initial color at $\vec{r}(\rho_{\mathrm{out}})$. The contraction of the Bloch sphere is more pronounced on the equatorial plane which shows that the main noise process is phase damping, as descried by the Hamiltonian of Eq. (1). There is also a rotation of the sphere around the $|1\rangle - |2\rangle$ axis at a rate of ~9° sec^{-1} due to small inaccuracies in the control field.

The decay of the coherence with a DD pulse sequence and assuming a Gaussian phase distribution is given in a system-reservoir framework by [19,31]

$$C(t) = e^{-\int_0^\infty d\omega S_\delta(\omega)F(\omega t)/\pi\omega^2}, \qquad (2)$$

where the argument is the overlap integral between the fluctuations power spectrum, $S_\delta(\omega) = \int_{-\infty}^{\infty}\langle\delta(t)\delta(0)\rangle \times e^{i\omega t}dt$, and a filter function which encapsulates the information on the DD pulse sequence and is given by $F(\omega t) = \frac{1}{2}|\sum_{k=0}^{n}(-1)^k(e^{i\omega t_{k+1}} - e^{i\omega t_k})|^2$ with $t_0 = 0$ and $t_{n+1} = t$. For each atom $\delta(t)$ is a sequence of constant detunings connected by "jumps" which occur after each collision. Since the collision times follow Poisson statistics, the

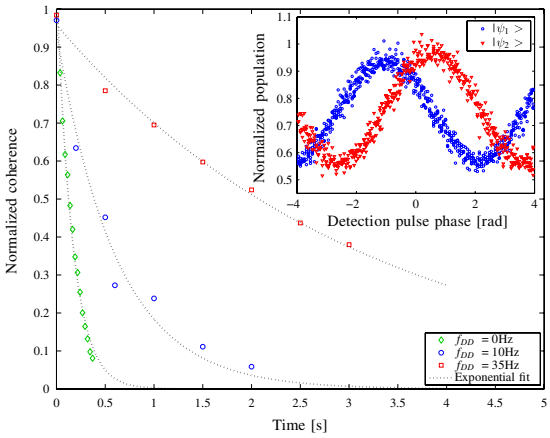

FIG. 3 (color online). The ensemble coherence versus time without DD ($f_{\mathrm{DD}} = 0$ Hz) and with two representing DD pulse rates, normalized to the initial coherence. The inset shows a storage of two orthogonal initial states in the equatorial plane: $|\psi_1\rangle = (1/\sqrt{2})(|1\rangle + |2\rangle)$ and $|\psi_2\rangle = (1/\sqrt{2})(|1\rangle + e^{i\pi/2}|2\rangle)$. We add to the decoupling scheme another pulse independent of the initial state with a phase and duration chosen to correct for the small rotation of the Bloch sphere as was measured in the QPT. We measure the population at $|2\rangle$ after 3 sec, normalized to the initial population, versus the phase of a $\pi/2$ detection pulse. The fringe contrast is not centered to 0.5 due to inelastic m-changing transitions.

detuning correlation function decays exponentially, $\Phi_\delta(t) = \langle\delta(t+0)\delta(0)\rangle = \sigma_\delta^2 e^{-\Gamma|t|}$, where Γ^{-1} is the correlation time of the detuning and σ_δ is the standard deviation of the detunings distribution. The power spectrum is given by $S_\delta(\omega) = \int_{-\infty}^{\infty}\Phi_\delta(t)e^{i\omega t}dt = 2\Gamma\sigma_\delta^2/(\Gamma^2+\omega^2)$. By solving numerically Eq. (2) and leaving the $\{t_i\}_{i=1}^n$ as free parameters, we find that the optimal decoupling sequence for a Lorentzian power spectrum is given by $t_i = \frac{\eta+i-1}{n-1+2\eta}t$, where $i = 1\ldots n$ and $0.5 \le \eta \le 1$ is a numerical factor which depends on n and t. For $\frac{\Gamma t}{n} \ll 1$ we find $\eta \approx 0.5$, for which we retrieve the CPMG pulse sequence. Furthermore, even when $\frac{\Gamma t}{n} \approx 1$ the coherence time with the CPMG pulse sequence differs by less than 1% from the optimal value. We have tested theoretically and experimentally other DD schemes, in particular, the one suggested in Ref. [18], and verified that they are indeed inferior to the CPMG sequence in our Lorentzian fluctuations power spectrum (for more details see the supplementary material [27]).

We measure $C(t)$ directly by preparing the atoms in the superposition $|\psi\rangle = \frac{1}{\sqrt{2}}(|1\rangle + |2\rangle)$, employ the DD pulse sequence, and finally measure the length of the Bloch vector with a quantum state tomography. Though $C(t)$ does not have to follow, *a priori*, some well defined function, the experimental results depicted in Fig. 3 show that the data are well fitted by an exponentially decaying function e^{-t/τ_c}, from which we extract the coherence time τ_c. The exponential decay is expected in the Markovian limit, where the decay time scale is much larger than the fluctuations correlation time [19]. A measurement of the dependence of the coherence time on the DD pulse rate is shown in Fig. 4. We observe a quadratic increase of the coherence time versus f_{DD} up to 35 Hz, for which there is a 20-fold improvement to more than 3 sec. For such long times the effect of inelastic collisions (T_1) already becomes significant, and at higher pulse rates the coherence time even decreases probably due to imperfections in the control pulses.

In order to explain these results we present a qualitative model for the coherence time. Without collisions the inhomogeneous dephasing rate is proportional to σ_δ. For simplicity we assume that if a collision did not occur between two consecutive π pulses the inhomogeneous broadening is averaged out. If a collision occurred, however, the width of the ensemble phase distribution increases by $\sim f_{\mathrm{DD}}^{-1}\sigma_\delta$. The number of collisions up to a time t is $\Gamma_{\mathrm{col}}t$, and since we add random variables (i.e., the accumulated phase), the width of the phase distribution increases as a square root of time: $\Delta\Phi(t) \sim f_{\mathrm{DD}}^{-1}\sigma_\delta\sqrt{\Gamma_{\mathrm{col}}t}$. For cold collisions in a three-dimensional (3D) harmonic trap, the relation between the collision rate and the relaxation rate was shown to be $\Gamma_{\mathrm{col}} = 2.7\cdot\Gamma$ [32]. The coherence time, τ_c, is the time for which the width of phase distribution is on the order of 1, yielding

$$\tau_c \sim f_{\mathrm{DD}}^2\sigma_\delta^{-2}\Gamma^{-1}, \tag{3}$$

with a parabolic dependence on f_{DD}. This result can be also obtained from Eq. (2) by approximating $\frac{F(\omega t)}{\pi(\omega t)^2} \approx \delta_{\mathrm{Dirac}}(\omega t - 2\pi f_{\mathrm{DD}}t)$ and using the Lorentzian power spectrum.

Exact calculations of τ_c using Eq. (2) without fitting parameters are presented in Fig. 4 in good agreement with the experimental data. The calculations are done with a Lorentzian power spectrum where the parameters Γ and σ_δ are extracted from measured quantities. Γ is extracted from the collision rate which is calculated using the measured temperature, number of atoms, and trap oscillation frequencies. The parameter σ_δ is measured in a Ramsey experiment at very low densities, where the collisions can be disregarded and σ_δ can be extracted from the measured dephasing rate [27]. We also perform Monte Carlo simulations, where we solve for the classical motion of atoms in the trap including collisions, and calculate the Ramsey signal by tracing each atom's accumulated phase along its trajectory. The results of the simulations are also depicted in Fig. 4, and agree well with both theory and experiments. We conclude that the effect of collisions can be indeed formulated as an effective single spin Hamiltonian coupled to a reservoir. Moreover, although the detunings of atoms trapped in a 3D harmonic trap are not normally distributed [27], the distribution of their accumulated phase can be well approximated by a

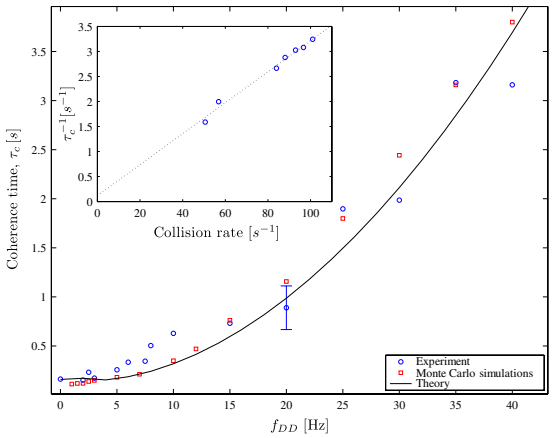

FIG. 4 (color online). The coherence time versus the dynamical decoupling pulse rate f_{DD}. The experimental data (blue circles) agree well both (i) with the theoretical prediction of Eq. (2) taking a Lorentzian power spectrum (solid line) with $\sigma_\delta = 23.8\ \mathrm{sec}^{-1}$ and $\Gamma = 37.5\ \mathrm{sec}^{-1}$ which were extracted from measured quantities and with no fit parameters and (ii) with molecular dynamics Monte Carlo simulations done with 1000 atoms in a 3D harmonic trap with an inhomogeneous decay time similar to the experiment (red squares). The error bar is estimated from the fits shown in Fig. 3. The inset shows a measurement of the dephasing rate for different collision rates for $f_{\mathrm{DD}} = 8$ Hz, demonstrating the linear dependence of Eq. (3). The dotted line is a linear fit of the data.

Gaussian owing to the central limit theorem and the large number of collisions involved.

Another prediction of Eq. (3) is the linear dependence of the coherence time on Γ^{-1}. In the experiment we change Γ by reducing the density and collision rate while keeping the temperature, and therefore σ_δ, unchanged [26]. This is accomplished by reducing the intensity of the cooling lasers in the trap loading stage. In the inset of Fig. 4 we plot τ_c^{-1} versus the average collision rate for a pulse rate of $f_{\mathrm{DD}} = 8$ Hz. As expected, the coherence time is inversely proportional to the collision rate.

In conclusion, we have demonstrated that dynamical decoupling can substantially reduce collisional decoherence in a dense atomic ensemble. In the current work the ensemble was treated as an effective single spin system which accounts for storage schemes based on collinear electromagnetically induced transparency [2]. A natural extension is the application of dynamical decoupling to W-type joint quantum states which are produced in Raman scattering schemes [1,3]. Another promising prospect lies in novel hybrid approaches to quantum computation combining atomic ensembles and superconducting devices [33], where the application of dynamical decoupling could reduce the error probability during the characteristic 100 μs single-qubit gate to less than 10^{-4}—below the current estimated threshold for a fault-tolerant quantum computation.

We thank Roee Ozeri, Guy Bensky, Goren Gordon, Gershon Kurizki, and Rami Pugatch for helpful discussions. We acknowledge the financial support of MIDAS, MINERVA, ISF, and DIP.

[1] L. M. Duan *et al.*, Nature (London) **414**, 413 (2001).
[2] M. D. Lukin, Rev. Mod. Phys. **75**, 457 (2003).
[3] A. Kuzmich *et al.*, Nature (London) **423**, 731 (2003).
[4] C. W. Chou *et al.*, Nature (London) **438**, 828 (2005).
[5] Z. Yuan *et al.*, Nature (London) **454**, 1098 (2008).
[6] B. Zhao *et al.*, Nature Phys. **5**, 95 (2009).
[7] U. Schnorrberger *et al.*, Phys. Rev. Lett. **103**, 033003 (2009).
[8] R. Zhang, S. R. Garner, and L. V. Hau, Phys. Rev. Lett. **103**, 233602 (2009).
[9] R. Grimm, M. Weidemuller, and Y. B. Ovchinnikov, Adv. At. Mol. Phys. **42**, 95 (2000).
[10] D. M. Harber *et al.*, Phys. Rev. A **66**, 053616 (2002).
[11] S. E. Harris and L. V. Hau, Phys. Rev. Lett. **82**, 4611 (1999).
[12] A. V. Gorshkov *et al.*, Phys. Rev. Lett. **98**, 123601 (2007).
[13] E. L. Hahn, Phys. Rev. **80**, 580 (1950).
[14] M. F. Andersen, A. Kaplan, and N. Davidson, Phys. Rev. Lett. **90**, 023001 (2003).
[15] L. Viola and S. Lloyd, Phys. Rev. A **58**, 2733 (1998).
[16] L. Viola, E. Knill, and S. Lloyd, Phys. Rev. Lett. **82**, 2417 (1999).
[17] C. Search and P. R. Berman, Phys. Rev. Lett. **85**, 2272 (2000).
[18] G. S. Uhrig, Phys. Rev. Lett. **98**, 100504 (2007).
[19] Ł. Cywinski *et al.*, Phys. Rev. B **77**, 174509 (2008).
[20] E. M. Fortunato *et al.*, New J. Phys. **4**, 5 (2002).
[21] E. Fraval, M. J. Sellars, and J. J. Longdell, Phys. Rev. Lett. **95**, 030506 (2005).
[22] J. J. L. Morton *et al.*, Nature Phys. **2**, 40 (2006).
[23] S. Damodarakurup *et al.*, Phys. Rev. Lett. **103**, 040502 (2009).
[24] M. J. Biercuk *et al.*, Nature (London) **458**, 996 (2009).
[25] J. Du *et al.*, Nature (London) **461**, 1265 (2009).
[26] S. Kuhr *et al.*, Phys. Rev. A **72**, 023406 (2005).
[27] See supplementary material at http://link.aps.org/supplemental/10.1103/PhysRevLett.105.053201 for more information regarding the experimental setup, quantum state, and process tomography, dephasing in a 3D harmonic trap and optimal DD sequence for a Lorentzian spectral function.
[28] L. Khaykovich et al., Europhys. Lett. **50**, 454 (2000).
[29] L. M. K. Vandersypen and I. L. Chuang, Rev. Mod. Phys. **76**, 1037 (2005).
[30] A. Widera *et al.*, New J. Phys. **8**, 152 (2006).
[31] G. Gordon, G. Kurizki, and D. A. Lidar, Phys. Rev. Lett. **101**, 010403 (2008).
[32] C. R. Monroe *et al.*, Phys. Rev. Lett. **70**, 414 (1993).
[33] D. Petrosyan *et al.*, Phys. Rev. A **79**, 040304 (2009).